Talanta 85 (2011) 964–969

Contents lists available at ScienceDirect

Talanta

journal homepage: www.elsevier.com/locate/talanta

Copper nanoparticles entrapped in SWCNT-PPy nanocomposite on Pt electrode as NO_x electrochemical sensor

Subash Prakash[a], Seenivasan Rajesh[b,1], Sushil Kumar Singh[c], Kalpana Bhargava[d], Govindaswamy Ilavazhagan[d], Veerapandy Vasu[e], Chandran Karunakaran[b,*]

[a] Department of Physics, VHNSN College, Virudhunagar 626001, India
[b] Biomedical Research Laboratory, Department of Chemistry, VHNSN College, Virudhunagar 626001, India
[c] Si-MEMS Division, Solid State Physics Laboratory (SSPL), New Delhi 110054, India
[d] Peptide and Proteomics Division, Defence Institute of Physiology and Allied Sciences (DIPAS), New Delhi 110054, India
[e] School of Physics, Madurai Kamaraj University, Madurai 625021, India

ARTICLE INFO

Article history:
Received 18 February 2011
Received in revised form 2 May 2011
Accepted 4 May 2011
Available online 13 May 2011

Keywords:
NO_x electrochemical sensor
Copper nanoparticles
Single-walled carbon nanotube
Polypyrrole matrix

ABSTRACT

A highly sensitive NO_x sensor was designed and developed by electrochemical incorporation of copper nanoparticles (CuNP) on single-walled carbon nanotubes (SWCNT)-polypyrrole (PPy) nanocomposite modified Pt electrode. The modified electrodes were characterized by scanning electron microscopy and energy dispersive X-ray analysis. Further, the electrochemical behavior of the CuNP-SWCNT-PPy-Pt electrode was investigated by cyclic voltammetry. It exhibited the characteristic CuNP reversible redox peaks at −0.15 V and −0.3 V vs. Ag/AgCl respectively. The electrocatalytic activity of the CuNP-SWCNT-PPy-Pt electrode towards NO_x is four-fold than the CuNP-PPy-Pt electrode. These results clearly revealed that the SWCNT-PPy nanocomposite facilitated the electron transfer from CuNP to Pt electrode and provided an electrochemical approach for the determination of NO_x. A linear dependence ($r^2 = 0.9946$) on the NO_x concentrations ranging from 0.7 to 2000 μM, with a sensitivity of 0.22 ± 0.002 μA μM^{-1} cm^{-2} and detection limit of 0.7 μM was observed for the CuNP-SWCNT-PPy-Pt electrode. In addition, the sensor exhibited good reproducibility and retained stability over a period of one month.

1. Introduction

Nitric oxide (NO) plays a vital role in the normal vascular biology and pathophysiology [1]. NO, a neuronal signaling molecule in the central and peripheral nervous system can be synthesized by mammalian cells. Further it acts as a physiological messenger and cytotoxic agent [2,3]. It is very unstable with a half-life of 2–30 s and rapidly reacts with molecular oxygen to form NO_x (NO and NO_2) [4]. Therefore, sensitive and accurate methods for the determination of NO_x are required.

Many methods for the determination of NO_x have been proposed [5], such as electron paramagnetic resonance [6], spectrophotometry [7] and chemiluminescence [8]. Among them, electrochemical techniques are proved to be powerful tools due to their advantages of simplicity, portability, inexpensive and fast analysis [9,10]. Several reports are available on the detection of NO_x using the resistive [11,12], potentiometric [13–15] or amperometric [16,17] methods. Recently, the ZnO–In_2O_3 films have been widely used for detecting NO_x gas [18]. However, the sensor, lacked high sensitivity and operated at high temperature (200–500 °C) [19,20].

Carbon nanotubes (CNTs) have been widely used in sensor because they posses good chemical stability, and excellent electronic and mechanical properties [21–23]. These unique properties make CNTs very useful for supporting inorganic nanomaterials, such as copper nanoparticle (CuNP) which can be used as an electrochemical sensor [24]. CNTs have high conductivity and large surface area which would greatly promote the performance of CuNP. Direct formation of CuNPs onto CNTs has the advantage that inherent properties of the nanocrystals and nanotubes are preserved [25].

However nanoparticles and CNT incorporation on the electrode surface is a major hurdle. Recently, there has been wide interest in the field of conducting polymer modified electrodes as it exhibited more porous structure [26,27]. Among the conducting polymers, polypyrrole (PPy) [28] matrix increases the rates of reaction occurring at the electrode surface by mediating the electron transport and also the surface area. Conductive PPy polymer matrix has proven effective at electrically wiring the CNTs to the underlying electrode [29]. Electrodes modified with SWCNT-PPy nanocomposite reported by us exhibited good performances, such as catalysis, enhancement of mass transport, high effective

* Corresponding author. Tel.: +91 9486431953; fax: +91 04562 281338.
E-mail address: ckaru2000@gmail.com (C. Karunakaran).
[1] Present position: Department of Bio-Technology, Mepco Schlenk Engineering College, Sivakasi 626005.

0039-9140/$ – see front matter © 2011 Elsevier B.V. All rights reserved.
doi:10.1016/j.talanta.2011.05.004

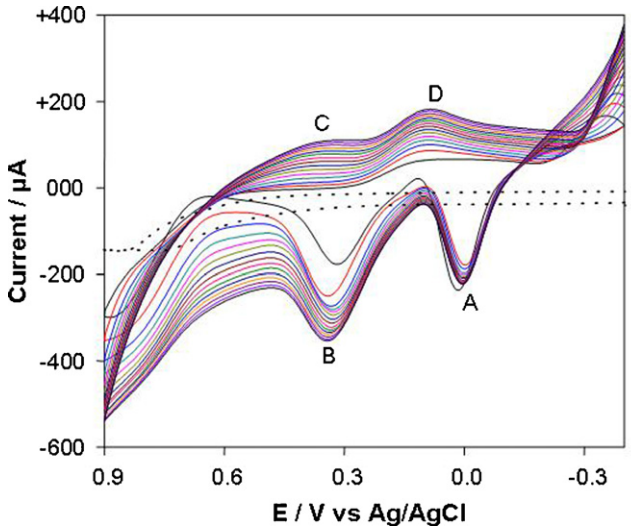

Fig. 1. Continuous (solid) lines show the CV obtained by cycling electrodeposition of CuNP on SWCNT-PPy-Pt electrode in 0.1 M KCl as supporting electrolyte; potential range from −0.4 to +0.9 V vs. Ag/AgCl for 15 complete cycles (from inner to outer); scan rate: 50 mV s^{-1}. Dotted line shows the CV of PPy on Pt electrode in the same supporting electrolyte.

surface area, and good biocompatibility [27]. Moreover, the Cu nanoparticles modified electrodes are favored as electrochemical catalyst for the detection of NO molecules because of their high electrical conductivity and redox catalytic activity similar to copper containing enzymes.

So, in this study we investigated for first time the CuNP incorporated on SWCNT-PPy nanocomposite modified Pt electrode for the determination of NO_x. This sensor electrode exhibited good electrochemical response for the determination of NO_x.

2. Experimental

2.1. Reagents

Pyrrole, sodium nitrite ($NaNO_2$), and diethylenetriaminepentaacetic acid (DTPA) were purchased from Sigma–Aldrich Company, USA. Pyrrole was used without purification.

2.2. Instrumentations

All electrochemical experiments were performed on CHI 2000A electrochemical workstation (CHI, USA) with a conventional three electrode system which consisted of an Ag/AgCl wire as reference electrode, a Pt wire as auxiliary or counter electrode, and a CuNP-SWCNT-PPy-Pt as the working electrode. The size of Pt wire working electrode was 0.5 mm in diameter. The morphological scanning electron microscopic (SEM) images and energy dispersive X-ray analysis (EDX) spectrum were obtained using a FEI Quanta FEG 200-High Resolution Scanning Electron Microscope (FEI Co. Netherlands)

2.3. Fabrication of NO_x sensor

Prior to the experiment, the Pt electrode of 0.5 mm diameter was polished with alumina powder (size 0.05 and 1.0 μm) and washed twice with double distilled water. The cleaned Pt electrode was pretreated with 1 M H_2SO_4 by scanning the potential from −0.2 to +1.45 V for 10 cycles and then washed with double distilled water. This pretreatment was employed before each electropolymerization of pyrrole.

SWCNT entrapped PPy matrix on Pt electrode was prepared by a two-step procedure. First, PPy films were polymerized on Pt electrode according to the published report [30]. Briefly, the irreversible oxidation of 0.4 M pyrrole in 0.1 M KCl occurred in the potential range from 0 to +0.9 V vs. Ag/AgCl electrode for 10 complete cycles under argon atmosphere. The optimum of 10 cycles for pyrrole electropolymerization was used because of its increased conductivity and surface area as reported earlier [31,32]. Then, the SWCNT modified PPy-Pt electrode was prepared by the reported procedure [33]. In brief, 25 μl of SWCNT solution (1 ml of 0.5 wt% nafion–ethanol solution containing 2 mg of SWCNT) was dropped on PPy-Pt electrode surface, and then the solvent ethanol was evaporated in air to form a SWCNT-PPy nanocomposite. Then, CuNP were electrochemically deposited on SWCNT-PPy-Pt electrode from a $CuCl_2$ (0.1 M) solution by applying the potential from −0.4 to +0.9 V vs. Ag/AgCl in the presence of 0.1 M KCl as supporting electrolyte [34]. The stepwise fabrication of NO_x sensor and the reaction mechanism occurring at the surface of the sensor during the determination of NO_x is illustrated in Scheme 1.

The CuNP-SWCNT-PPy-Pt electrode was characterized by SEM, EDX spectrum and cyclic voltammetry. The surface coverage of electroactive CuNP on SWCNT-PPy-Pt electrode was determined by integration of the peak area under the anodic/cathodic CuNP cyclic voltammetric peaks obtained in 0.1 M phosphate buffer solution (PBS).

2.4. Sample preparation

NO_x was prepared according to the following Eq. (1). NO_x was generated based on the stoichiometric reaction in the presence of air [35].

$$NaNO_2 + H_2SO_4 \xrightarrow{O_2} NO_x \uparrow + H_2O + Na_2SO_4 \quad (1)$$

Since the conversion of NO_2^- to NO_x is stoichiometric, the final concentration of NO_x generated is equal to the concentration of $NaNO_2$ in the solution [36].

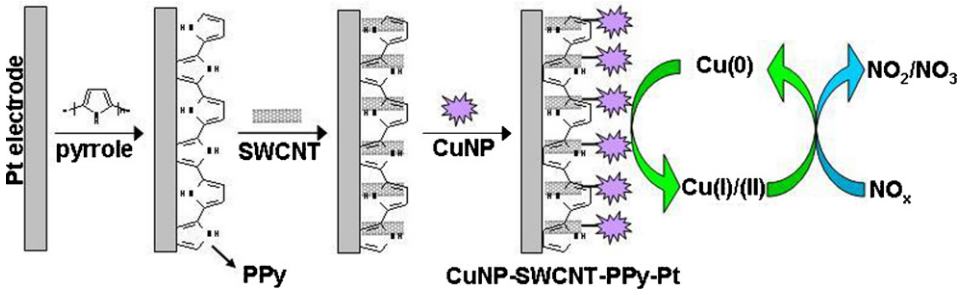

Scheme 1. Schematic stepwise preparation of the CuNP-SWCNT-PPy-Pt electrode and illustration of the reaction processes occurring at the surface of the sensor during the determination of NO_x.

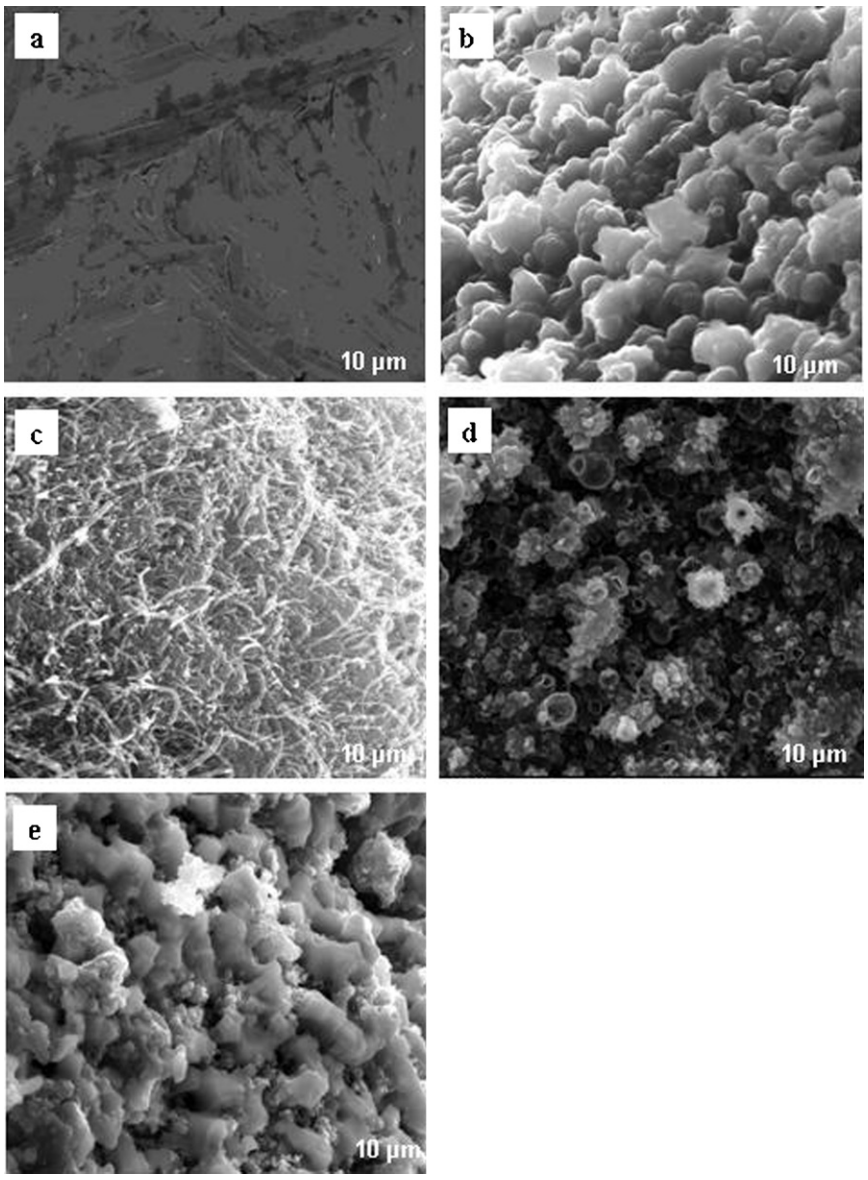

Fig. 2. SEM micrographs of (a) bare Pt, (b) PPy-Pt, (c) SWCNT-PPy-Pt, (d) CuNP-PPy-Pt and (e) CuNP-SWCNT-PPy-Pt electrodes.

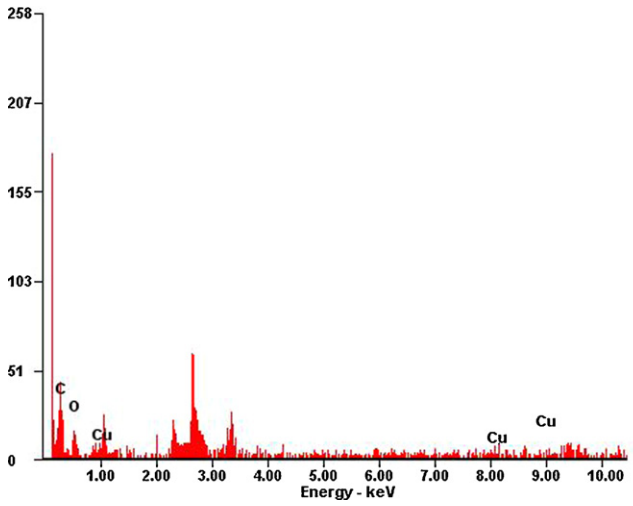

Fig. 3. EDX spectrum for CuNP-SWCNT-PPy-Pt electrode.

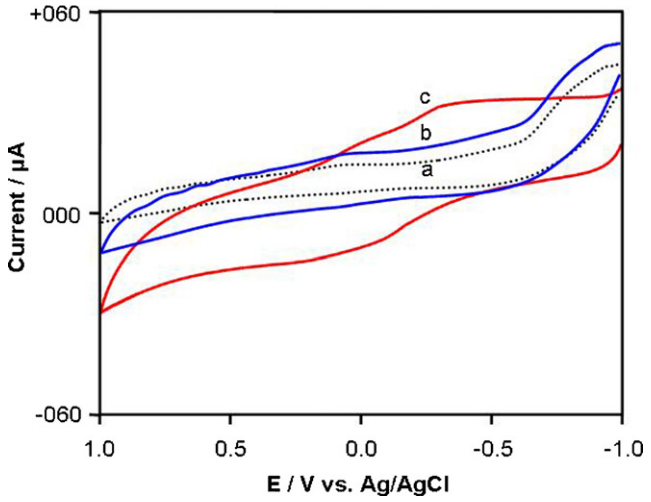

Fig. 4. Typical CV responses of (a) PPy-Pt, (b) SWCNT-PPy-Pt and (c) CuNP-SWCNT-PPy-Pt electrodes in 0.1 M PBS; scan rate: 50 mV s^{-1} vs. Ag/AgCl.

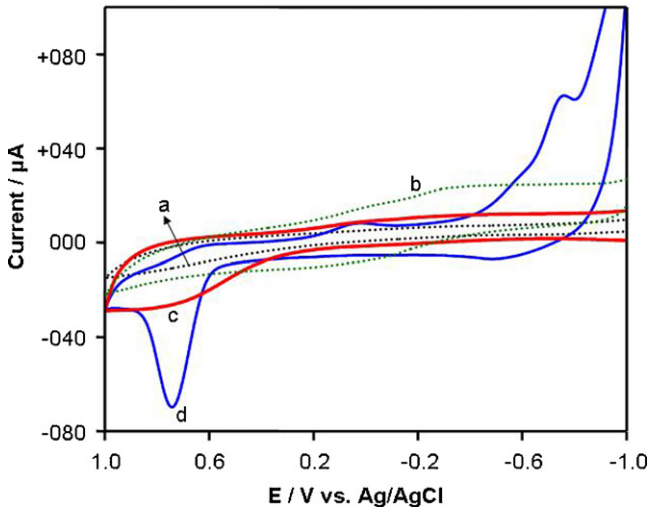

Fig. 5. Electrochemical response of SWCNT-PPy-Pt and CuNP-SWCNT-PPy-Pt electrodes (dotted) in the absence (a and b) of; (solid) in the presence (c and d) of 500 μM NO_x solution in 0.1 M PBS; scan rate: 50 mV s^{-1} vs. Ag/AgCl.

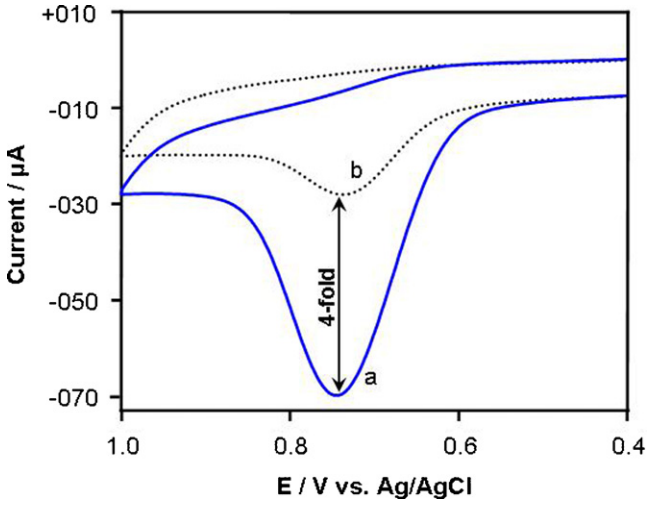

Fig. 6. Influence of SWCNT on CV responses of (a) CuNP-SWCNT-PPy-Pt and (b) CuNP-PPy-Pt electrodes in 0.1 M PBS containing 500 μM NO_x; scan rate: 50 mV s^{-1} vs. Ag/AgCl.

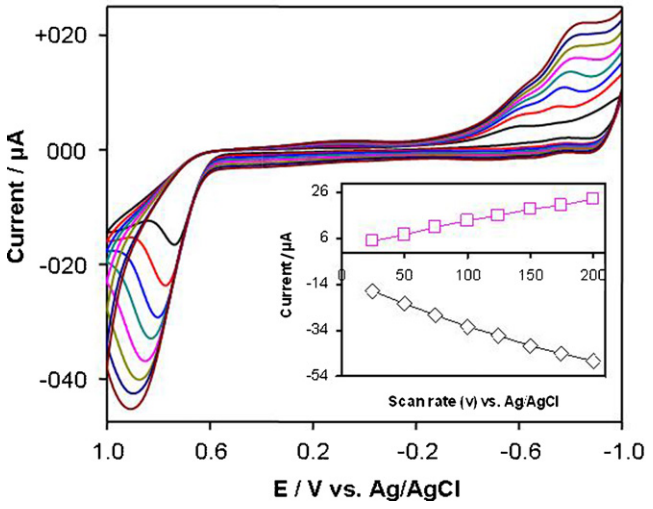

Fig. 7. Typical CV response of CuNP-SWCNT-PPy-Pt electrode at different scan rate in 0.1 M PBS containing 500 μM NO_x; scan rates from 25, 50, 75, 100, 150, 200, 250, 300 mV s^{-1}. Inset: A linear calibration plot of anodic and cathodic peak current vs. scan rate.

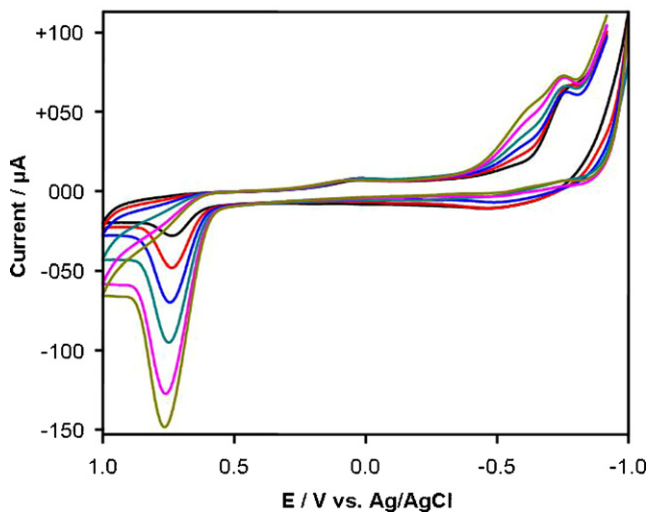

Fig. 8. Typical CV response of CuNP-SWCNT-PPy-Pt electrode in 0.1 M PBS containing (a) 100 μM, (b) 250 μM, (c) 500 μM, (d) 1000 μM, (e) 1500 μM and (f) 2000 μM NO_x at scan rate of 50 mV s^{-1} vs. Ag/AgCl.

3. Results and discussion

3.1. Electrochemical deposition of CuNP

In Fig. 1, the dotted line shows the cyclic voltammograms (CV) of electropolymerized pyrrole on Pt electrode in 0.1 M KCl as supporting electrolyte. The CV of the electrodeposition of CuNP on SWCNT-PPy-Pt electrode with successive sweeps between −0.4 and +0.9 V for 15 cycles are shown in Fig. 1 (solid line). During the electrodeposition of CuNP, the CV exhibit well defined redox peaks A–D. The peak 'A' corresponds to the oxidation of Cu(0) to Cu(I). The peaks B and C are ascribed to the complex occurred between the deposited copper (I)/(II) and SWCNT-PPy [34]. The peak D is due to Cu(II)/Cu(I) reductions [33]. However, the PPy-Pt electrode showed no effective peaks due to A–D. These results confirmed that the CuNP was entrapped in SWCNT-PPy matrix.

3.2. Characterization of CuNP-SWCNT-PPy-Pt electrode

The surface morphological images of bare Pt, PPy-Pt, SWCNT-PPy-Pt, CuNP-PPy-Pt and CuNP-SWCNT-PPy-Pt electrodes were obtained as shown in Fig. 2(a–e). Fig. 2(b) shows the typical highly microporous morphology of PPy on Pt electrode surface. SWCNT

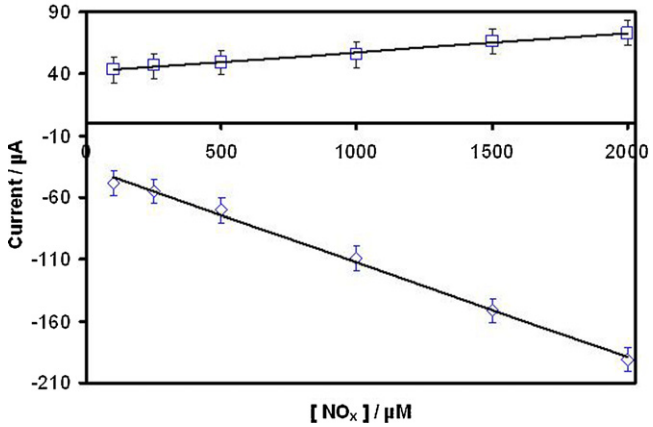

Fig. 9. A linear calibration plot of anodic and cathodic peak currents against NO_x concentrations (each point represents the three repetitive measurements).

Table 1
Comparison of linear range, detection limit and sensitivity with different NO sensors.

Electrode	E_{app} (V)	Linear range (μM)	Detection limit (μM)	Sensitivity (μA μM^{-1} cm^{-2})	Ref.
Hb/MMT/PVA/PGE	−0.783	1–250	0.5	–	[38]
PGE/Mn(III) protoporphyrin IX	−0.85	0.5–50	–	–	[39]
Hb/Au-CPE	−1.0	0.9–300	0.1	–	[40]
Nf/NiTSPc/GCE	–	Up to 3.6	–	0.0066	[41]
PTTCA/Cyt-c/Pt	–	2.4–55	0.013	0.117	[42]
CuNP-SWCNT-PPy-Pt	+0.78	0.7–2000	0.7	0.22 ± 0.002	This work

Au, gold; CPE, carbon paste electrode; Cyt-c, cytochrome c; GCE, glassy carbon electrode; Hb, hemoglobin; MMT, montmorillonite; Nf, nafion; NiP, Tetrakis (3-methoxy-4-hydroxyphenyl) nickel(II) porphyrin; NiTSPc, nickel tetrasulfonated phthalocyanine; PGE, pyrolytic graphite electrode; Pt, platinum; PTTCA-5,2, poly 5,2-terthiophene-3-carboxylic acid; PVA, polyvinyl alcohol.

was found to be immobilized in the PPy matrix and formed the nanocomposite as shown in Fig. 2(c). Fig. 2(d) clearly exhibits the deposition of CuNP on PPy. Further, Fig. 2(e) shows the effective incorporation of CuNP on highly microporous nature of SWCNT-PPy matrix than that of PPy matrix. A representative EDX spectrum for the CuNP-SWCNT-PPy-Pt electrode was given in Fig. 3. In this spectrum, Cu and O peaks reveals the presence of CuNP in the SWCNT-PPy-Pt electrode.

3.3. Electrochemical characterization

The cyclic voltammetric responses of the CuNP-SWCNT-PPy-Pt, SWCNT-PPy-Pt and PPy-Pt electrodes in 0.1 M PBS at a scan rate of 50 mV s^{-1} are shown in Fig. 4. Fig. 4(a and b) exhibits the CV peaks of PPy-Pt and SWCNT-PPy-Pt electrodes showing no characteristic redox peaks. Fig. 4(c) shows a pair of characteristics redox peaks of CuNP at −0.15 V (anodic peak) and −0.3 V (cathodic peak) indicating the presence of CuNP on SWCNT-PPy-Pt electrode. Difference of the anodic and cathodic peak potential values was ΔE = 0.15 V, whereas formal potential (an average midpoint potential of cathodic and anodic peak potential) for CuNP redox reaction on the electrode was −0.225 V.

3.4. Electrochemical response of electrodes for NO_x sensing

The CVs of the SWCNT-PPy-Pt and CuNP-SWCNT-PPy-Pt electrodes in 0.1 M PBS in the applied potential range from −1.0 to +1.0 V at a scan rate of 50 mV s^{-1} in the absence of NO_x are displayed in Fig. 5(a and b). Upon addition of 500 μM of NO_x into the 0.1 M PBS, a new irreversible anodic oxidation peak appeared at about +0.78 V (Fig. 5(d)) for the CuNP-SWCNT-PPy-Pt electrode, which may be attributed to the oxidation of NO_x. But, without CuNP in the modified electrode under the same condition in the presence of NO_x, there was only a very small change observed at about +0.78 V (Fig. 5(c)). This study clearly demonstrates the electrocatalytic anodic oxidation of NO_x by CuNP on SWCNT-PPy-Pt.

The effect of SWCNT on the current response due to NO_x is shown in Fig. 6. In the presence of NO_x (500 μM), the anodic oxidation current was increased four-fold in the CuNP-SWCNT-PPy-Pt electrode (Fig. 6(a)) than that of the CuNP-PPy-Pt electrode (Fig. 6(b)). It is perhaps due to the SWCNT-PPy nanocomposite providing large surface area for enhanced loading of CuNP and facilitating the direct electron transfer between CuNP and the Pt electrode.

3.5. Effect of scan rate with respect to NO_x

For the investigation of reaction mechanism, typical CV response of NO_x in 0.1 M PBS on CuNP-SWCNT-PPy-Pt electrode was studied at different scan rates as shown in Fig. 7. Inset shows the effect of scan rate (ν) vs. the anodic and cathodic peak currents for 500 μM NO_x. According to the theoretical model of Andrieux and Saveant [37], the catalytic current I_p depends on the potential scan rates (ν) as follows in Eq. (2):

$$I_p = 0.496FAC_oD_o^{1/2}\left(\frac{F\nu}{RT}\right)^{1/2} \quad (2)$$

where C_o is the analyte concentration, D_o represents the diffusion coefficient of the analyte, Faraday constant (F), gas constant (R) and temperature (T). The anodic and cathodic peak currents of NO_x were thus linearly related to the square root of scan rate in the range of 25–300 mV s^{-1} indicating the catalytic oxidation of NO_x as a diffusion-controlled process.

3.6. Effect of NO_x concentrations

Fig. 8 displays the typical catalytic current response at the CuNP immobilized on SWCNT-PPy-Pt electrode with the increase in the concentration of NO_x at 50 mV s^{-1}. A progressive increase in the current response was observed at +0.78 V with the increase in the concentrations of NO_x from 0.7 to 2000 μM as shown in Fig. 9. The anodic and cathodic peak currents of the modified electrode were almost linearly related to the concentrations of NO_x in the range of 0.7–2000 μM and the detection limit was 0.7 μM, with a sensitivity of 0.22 ± 0.002 μA μM^{-1} cm^{-2}. Without SWCNT, the CuNP-PPy-Pt electrode exhibited low sensitivity (0.012 ± 0.003 μA μM^{-1} cm^{-2}) for NO_x determination.

3.7. Selectivity, stability and reproducibility of CuNP-SWCNT-PPy-Pt electrode

The reproducibility of the present method for the determinations of NO_x was investigated in 0.1 M PBS containing 500 μM NO_x by repetitive determination of NO_x in triplicate. The results showed good reproducibility of the modified electrode, with a relative standard deviation of 3.2% for NO_x. For studying the stability of the sensor, the anodic and cathodic responses of NO_x was recorded three times daily and the current responses was found to be constant for at least 30 days. The good analytical properties of the sensor, such as low detection limit, long term stability, and high sensitivity, eventually have shown a great promise for the measurement of NO_x.

The time vs. current response of the sensor for the addition of 500 μM each of ascorbic acid and uric acid was studied (data not shown). When these interferences were added into the 0.1 M PBS containing 500 μM NO_x, there were no changes in the current. However, in the presence of 500 μM H_2O_2 we observed the anodic oxidation peak current at +0.10 V and cathodic reduction peak current at −0.31 V (data not shown). There is no significant interference at the NO_x potential +0.78 V leading to the selective determination of NO_x.

The electroanalytical properties of the present sensor was compared with the recently reported NO sensors and summarized in Table 1. It exhibited comparable detection limit, wide linearity and

with higher sensitivity than the reported sensors. Further, CuNP an enzyme mimetic is easy to prepare compared to metalloporphyrin and also devoid of enzyme fouling effects.

4. Conclusion

We report here for the first time CuNP entrapped in SWCNT-PPy nanocomposite on Pt electrode based sensor for the detection and measurement of NO_x. The modified CuNP-SWCNT-PPy-Pt electrode exhibited excellent electrocatalytic activity towards the oxidation and reduction of NO_x. It is perhaps due to the SWCNT-PPy nanocomposite providing large surface area for the effective loading of CuNP, an enzyme mimetic, and facilitating the direct electron transfer from CuNP to Pt electrode. The relatively good stability implies that the CuNP-SWCNT-PPy film is very stable and strongly bound to the Pt surface. Also, this modified electrode presented a number of attractive features for NO_x determination, such as simplicity in preparation, low detection limit, high sensitivity, selectivity and wide linear range, which attribute to the synergistic effect of CuNP and SWCNT.

Acknowledgements

Thanks are due to the Managing Board, VHNSN College, Virudhunagar and UGC, New Delhi for funding/providing facilities to carryout the research in the Biomedical Research Laboratory, VHNSN College, Virudhunagar, TamilNadu, India.

References

[1] S. Moncada, R.M. Palmer, E.A. Higos, Pharmacol. Rev. 43 (1991) 109–142.
[2] D.E. Koshland, Science 258 (1992) 1861–1862.
[3] J.P. Lei, H.X. Ju, O. Ikeda, J. Electroanal. Chem. 567 (2004) 331–338.
[4] L.J. Ignarro, J.M. Fukuto, J.M. Griscavage, N.E. Rogers, R.E. Byrns, Proc. Natl. Acad. Sci. U.S.A. 90 (1993) 8103–8107.
[5] M.J. Moorcroft, J. Davis, R.G. Compton, Talanta 54 (2001) 785–803.
[6] C.M. Arroyo, M. Kohno, Free Radical Res. Commun. 14 (1991) 145–155.
[7] M. Kelm, M. Feelisch, R. Spahr, H.M. Piper, E. Noack, J. Schrader, Biochem. Biophys. Res. Commun. 154 (1988) 236–244.
[8] T. Aoki, Biomed. Chromatogr. 4 (1990) 128–130.
[9] K. Shibuki, Neurosci. Res. 9 (1990) 69–76.
[10] C. Fan, G. Li, J. Zhu, D. Zhu, Anal. Chim. Acta 423 (2000) 95–100.
[11] Y. Yamada, M. Ogita, Sens. Actuators B 93 (2003) 546–551.
[12] A. Cabot, A. Marsal, J. Arbiol, J.R. Motante, Sens. Actuators B 99 (2004) 74–89.
[13] N. Miura, S. Zhuiykov, T. Ono, M. Hasei, N. Yamazoe, Sens. Actuators B 83 (2002) 222–229.
[14] N. Imanaka, A. Oda, S. Tamura, G. Adachi, J. Electrochem. Soc. 151 (2004) H113–H116.
[15] A. Dutta, N. Kaabbuathong, M.L. Grilli, E.Di. Bartolomeo, E. Traversa, J. Electrochem. Soc. 150 (2003) H33–H37.
[16] V. Coillard, L. Juste, C. Lucat, F. Menil, Meas. Sci. Technol. 11 (2000) 212–220.
[17] T. Nakamura, Y. Sakamoto, K. Saji, J. Sakata, Sens. Actuators B 93 (2003) 214–220.
[18] C.-Y. Lin, Y.-Y. Fang, C.-W. Linb, J.J. Tunney, K.-C. Hoa, Sens. Actuators B 146 (2010) 28–34.
[19] T. Becker, S. Muhlberger, B.C. Bosch-v, G. Muller, T. Ziemann, K.V. Hechtenberg, Sens. Actuators B 69 (2000) 108–119.
[20] J. Santos, P. Serrini, B. O'Beirn, L. Manes, Sens. Actuators B 43 (1997) 154–160.
[21] C.N.R. Rao, B.C. Satishkumar, A. Govindaraj, M. Nath, Chem. Phys. Chem. 2 (2001) 78–105.
[22] H.J. Dai, Acc. Chem. Res. 35 (2002) 1035–1044.
[23] P.M. Ajayan, Chem. Rev. 99 (1999) 1787–1799.
[24] H. Chu, L. Wei, R. Cui, J. Wang, Y. Li, Coord. Chem. Rev. 254 (2010) 1117–1134.
[25] L.A. Dobrzanski, M. Pawlyta, A. Krzton, B. Liszka, K. Labisz, J. Achiev. Mater. Manuf. Eng. 39 (2010) 184–189.
[26] S. Rajesh, U.S.E. Arivudainambi, S. Rajasingh, A. Rajendran, S. Kotamraju, C. Karunakaran, Sens. Lett. 8 (2010) 1–9.
[27] S. Rajesh, A.K. Kanugula, B. Kalpana, G. Ilavazhagan, S. Kotamraju, C. Karunakaran, Biosens. Bioelectron. 26 (2010) 689–695.
[28] M.E.G. Lyons, Analyst 119 (1994) 805–826.
[29] K. Balasubramanian, M. Burghard, Anal. Bioanal. Chem. 385 (2006) 452–468.
[30] N. Cioffi, N. Ditaranto, L. Torsi, R.A. Picca, E. De Giglio, L. Sabbatini, L. Novello, G. Tantillo, T. Bleve Zacheo, P.G. Zambonin, Anal. Bioanal. Chem. 382 (2005) 1912–1918.
[31] S.S. Razola, B.L. Ruiz, N.M. Diez, H.B. Mark, J.M. Kauffmann, Biosens. Bioelectron. 17 (2002) 921–928.
[32] N. Nagami, H. Umakoshi, T. Shimanouchi, R. Kuboi, Biochem. Eng. J. 21 (2004) 221–227.
[33] J. Wang, M. Musameh, Y. Lin, J. Am. Chem. Soc. 125 (2003) 2408.
[34] N. Cioffi, L. Torsi, I. Losito, C.D. Franco, I.D. Bari, L. Chiavarone, G. Scamarcio, V. Tsakova, L. Sabbatinia, P.G. Zambonin, J. Mater. Chem. 11 (2001) 1434–1440.
[35] H. Zhou, Y. Xu, T. Chen, I. Suzuki, G. Li, Anal. Sci. 22 (2006) 337–340.
[36] X. Zhang, Front. Biosci. 9 (2004) 3434–3446.
[37] C.P. Andrieux, J.M. Saveant, J. Electroanal. Chem. 93 (1978) 163–168.
[38] J. Pang, C. Fan, X. Liu, T. Chen, G. Li, Biosens. Bioelectron. 19 (2003) 441–445.
[39] C.Z. Li, S. Alwarappan, W. Zhang, N. Scafa, X. Zhang, Am. J. Biomed. Sci. 1 (2009) 274–282.
[40] Y. Xu, C. Hu, S. Hu, Sens. Actuators B 148 (2010) 253–258.
[41] S.C. Chang, N. Pereira-Rodrigues, J.R. Henderson, A. Cole, F. Bedioui, C.J. McNeil, Biosens. Bioelectron. 21 (2005) 917–922.
[42] W.C. Alvin Koh, M.A. Rahman, E.S. Choe, D.K. Lee, Y.-B. Shim, Biosens. Bioelectron. 23 (2008) 1374–1381.